Journal of Organometallic Chemistry 851 (2017) 225–234

Contents lists available at ScienceDirect

Journal of Organometallic Chemistry

journal homepage: www.elsevier.com/locate/jorganchem

Ruthenium(II) complexes of Schiff base derived from cycloalkylamines as pre-catalysts for ROMP of norbornene and ATRP of methyl methacrylate

Maria Beatriz A. Afonso [a], Thais R. Cruz [a], Yan F. Silva [a], João Clécio A. Pereira [b], Antonio E.H. Machado [c], Beatriz E. Goi [a], Benedito S. Lima-Neto [b], Valdemiro P. Carvalho-Jr [a, *]

[a] Faculdade de Ciências e Tecnologia, UNESP Univ Estadual Paulista, CEP 19060-900, Presidente Prudente, SP, Brazil
[b] Instituto de Química de São Carlos, Universidade de São Paulo, CEP 13560-970, São Carlos, SP, Brazil
[c] Instituto de Química, UFU Universidade Federal de Uberlândia, CEP 38400-902, Uberlândia, MG, Brazil

ARTICLE INFO

Article history:
Received 4 August 2017
Received in revised form
18 September 2017
Accepted 28 September 2017
Available online 30 September 2017

Keywords:
Schiff base
Ruthenium complexes
ROMP
ATRP
Norbornene
Methyl methacrylate

ABSTRACT

Ruthenium(II) complexes of Schiff base derived from cycloalkylamines (cycloalkyl = cyclopentyl (**1a**), cyclohexyl (**1b**), cycloheptyl (**1c**), and cyclooctyl) (**1d**) were synthesized: [RuCl(CyPen-Salen)(PPh_3)$_2$] (**2a**), [RuCl(CyHex-Salen)(PPh_3)$_2$] (**2b**), [RuCl(CyHep-Salen)(PPh_3)$_2$] (**2c**), and [RuCl(CyOct-Salen)(PPh_3)$_2$] (**2d**). The Schiff base-Ru^{II} complexes **2a-d** were characterized by elemental analysis, FTIR, UV-Vis, ^{1}H-, ^{13}C and ^{31}P NMR, and cyclic voltammetry. The complexes **2a-d** were evaluated as catalytic precursors for ROMP of norbornene (NBE) and for ATRP of methyl methacrylate (MMA). The syntheses of polynorbornene (polyNBE) via ROMP with complexes **2a-d** as pre-catalysts were evaluated under different reaction conditions ([HCl]/[Ru], [EDA]/[Ru], [NBE]/[Ru], and temperature). The highest yields of polyNBE were obtained with [NBE]/[HCl]/[Ru] = 5000/25/1 M ratio in the presence of 5 μL of EDA for 60 min at 50 °C. MMA polymerization via ATRP was conducted using the complexes **2a-d** in the presence of ethyl-α-bromoisobutyrate (EB*i*B) as initiator. The catalytic tests were evaluated as a function of the reaction time using the initial molar ratio of [MMA]/[EB*i*B]/[Ru] = 1000/2/1 at 85 °C. The linear correlation of $\ln([MMA]_0/[MMA])$ and time indicates that the concentration of radicals remains constant during the polymerization and that the ATRP of MMA mediated by **2a-d** proceeds in a controlled manner. Molecular weights increased linearly with conversion, however, the experimental molecular weights were higher than the theoretical ones.

1. Introduction

Schiff bases have been playing an important part in the development of coordination chemistry. Schiff base metal complexes have been studied extensively because of their attractive chemical and physical properties and their wide range of applications in numerous scientific areas [1–4]. Concurrently, complexes bearing Schiff base ligands are recognized as homogeneous or heterogeneous catalysts in various organic reactions. Schiff base complexes play a central role in various homogeneous catalytic reactions and the activity of these complexes varies with the type of ligands, coordination sites and metal ions. Furthermore, such complexes have recently attracted much attention for oxidation, epoxidation, hydrogenation, miscellaneous, and polymerization reactions [5,6].

In particular, notable works were conducted in ethylene polymerization reactions catalyzed by various metal complexes containing Schiff bases ligands. Aluminum complexes of a series of tridentate Schiff base ligands were found to catalyze the polymerization of ethylene [7]. A number of pyridyl bis(imide) complexes and phenoxy imine complexes are used as catalysts in the polymerization of ethylene [8,9]. Pyridine bis(imine) complexes of iron(III) and cobalt(II) show significant activity in the polymerization of ethylene and copolymerization of ethylene with 1-hexene [10]. The salicylaldiminato complexes of zirconium were found to be effective catalysts in ethylene polymerization and promoted radical decomposition in certain cases [11]. Poly(-methylmethacrylate) was prepared in presence of Cr(III) and Ni(II)

* Corresponding author.
E-mail address: valdemiro@fct.unesp.br (V.P. Carvalho-Jr).

https://doi.org/10.1016/j.jorganchem.2017.09.043
0022-328X/

salen complexes as catalysts for the controlled radical polymerization of methyl methacrylate (MMA) monomer [12]. Verpoort et al. reported a detailed discussion on catalytic activity in the atom transfer radical polymerization (ATRP) and ring opening metathesis polymerization (ROMP) of various substrates using Schiff bases Ru catalysts [13]. The critical points of these works showed that the efficiencies of catalysts were directly affected by the steric and electronic properties of the ligands. Therefore, the efforts in the easy synthesis of new catalysts and investigation of their activity in ROMP and ATRP reactions are an ongoing interest for the catalysis community.

Herein, we report the facile preparation and evaluation of novel ruthenium(II) complexes of bidentade Schiff bases derived from cycloalkylamines, where the cycloalkyl is cyclopentyl (**2a**), cyclohexyl (**2b**), cycloheptyl (**2c**), and cyclooctyl (**2d**) (Fig. 1), as pre-catalysts for ROMP of norbornene (NBE) and ATRP of methyl methacrylate (MMA) under different conditions of temperature, reaction time, and monomer concentration. Ethyl diazoacetate (EDA) was used as carbene source for ROMP and ethyl 2-bromoisobutyrate (EB*i*B) was used as initiator for ATRP. The goal was to observe the ring size influence and its effects on catalytic activity of the studies complexes, discussing the σ-donor ability and steric hindrance, obtaining resources to understand the factors that influence the efficiency of both reactions. Moreover, base Schiff ligands bound to ruthenium impart good stability and tolerance towards various organic functionalities, air and moisture, widening thus the area of their applications.

2. Experimental

2.1. General remarks

All reactions and manipulations were performed under nitrogen atmosphere following standard Schlenk techniques. 1,2-dichloroethane (DCE) was dried with $CaCl_2$ overnight, filtered, distilled and degassed by three vacuum–nitrogen cycles under nitrogen before use. Methyl methacrylate (MMA) was washed with 5% NaOH solution, dried over anhydrous $MgSO_4$, vacuum distilled from CaH_2 and stored under nitrogen at −18 °C before use. $RuCl_3.xH_2O$, 2,2,6,6-tetramethyl-1-piperidinoxyl (TEMPO), tetrabutylammonium hexafluorophosphate (n-Bu_4NPF_6), norbornene (NBE), ethyl diazoacetate (EDA), cyclopentylamine, cyclohexylamine, cycloheptylamine, cyclooctylamine, salicylaldehyde, and ethyl 2-bromoisobutyrate (EB*i*B) were used as acquired. The $[RuCl_2(PPh_3)_3]$ complex was prepared following the literature and its purity was checked by satisfactory elemental analysis and spectroscopic examination ($^{31}P\{^1H\}$ and ^1H NMR, FTIR and EPR) [14].

2.2. Analyses

Elemental analyses were performed with a Perkin-Elmer CHN 2400 at the Elemental Analysis Laboratory of Institute of Chemistry - USP. ESR measurements from solid sample were conducted at 77 K using a Bruker ESR 300C apparatus (X-band) equipped with a TE102 cavity and an HP 52152A frequency counter. The FTIR spectra in CsI pellets were obtained on a Bomem FTIR MB 102. Electronic spectra were recorded on a Varian model Cary 500 NIR spectrophotometer, using 1 cm path length quartz cells. The ^1H and $^{31}P\{^1H\}$NMR spectra were obtained in $CDCl_3$ at 298 K on a Bruker DRX-400 spectrometer operating at 400.13 and 161.98 MHz, respectively. The obtained chemical shifts were reported in ppm relative to TMS or 85% H_3PO_4. Conversion was determined from the concentration of residual monomer measured by gas chromatography (GC) using a Shimadzu GC-2010 gas chromatograph equipped with a flame ionization detector and a 30 m (0.53 mm I.D., 0.5 μm film thickness) SPB-1 Supelco fused silica capillary column. Anisole was added to polymerization and used as an internal standard. Analysis conditions: injector and detector temperature, 250 °C; temperature program, 40 °C (4 min), 20 °C min^{-1} until 200 °C, 200 °C (2 min). The molecular weights and the molecular weight distribution of the polymers were determined by gel permeation chromatography using a Shimadzu Prominence LC system equipped with a LC-20AD pump, a DGU-20A5 degasser, a CBM-20A communication module, a CTO-20A oven at 40 °C and a RID-10A detector equipped with two Shimadzu column (GPC-805: 30 cm, Ø = 8.0 mm). The retention time was calibrated with standard monodispersed polystyrene using HPLC-grade THF as an eluent at 40 °C with a flow rate of 1.0 mL min^{-1}. Electrochemical measurements were performed using an Autolab PGSTAT204 potentiostat with a stationary platinum disk and a wire as working and auxiliary electrodes, respectively. The reference electrode was Ag/AgCl. The measurements were performed at 25 °C ± 0.1 in CH_2Cl_2 with 0.1 mol L^{-1} of n-Bu_4NPF_6.

2.3. General procedure for the preparation of Schiff-Base Ligands (*1a-d*)

To prepare the Schiff base ligands **1a-d**, a solution of salicylaldehyde in methanol was slowly added over a solution of the respective cycloalkylamine in methanol. The mixture was stirred at room temperature for 16 h and the product was obtained as a yellowish orange oil. Any modifications are described below for each reaction.

Schiff-Base Ligand **1a**: Salicylaldehyde (0.48 g, 4.0 mmol), cyclopentylamine (0.34 g, 4.0 mmol), and methanol (15 mL) afforded 0.60 g (80%) of the title compound as a yellow oil. Refractive index 1.5626; (a) UV–Vis: $\lambda_{max(n)}$ (nm), $\varepsilon_{max(n)}$ [M^{-1} cm^{-1}]: $\lambda_{max(1)}$ (317), $\varepsilon_{max(1)}$ [9600]; (b) IR (KBr): ν_x (cm^{-1}): νC = N (1629), νC–O (1277); (c) ^1H NMR: ($CDCl_3$, 400 MHz): 13.8 (s, 1H, OH), 8.32 (s, 1H, CH=N), 7.27–7.31 ((dd, $^3J_{H,H}$ = 1.6 Hz, dd, $^3J_{H,H}$ = 0.8 Hz, 1H, salicyl-ring), 7.22–7.24 (dd, $^3J_{H,H}$ = 1.6 Hz, 1H, salicyl-ring), 6.93–6.96 (dt, $^3J_{H,H}$ = 6 Hz, $^3J_{H,H}$ = 0.4 Hz, 1H, salicyl-ring), 6.85–6.88 (td, $^3J_{H,H}$ = 0.8 Hz 1H, salicyl-ring), 3.75–3.82 (m, 1H, CH^{Pentyl}), 1.90–1.99 (m, 2H, CH_2^{Pentyl}), 1.81–1.88 (m, 2H, CH_2^{Pentyl}), 1.65–1.77 (m, 4H, CH_2^{Pentyl}),^{13}C NMR ($CDCl_3$) δ 162.3, 161.3, 131.8, 130.9, 118.4, 116.9, 70, 34.7, 24.5.

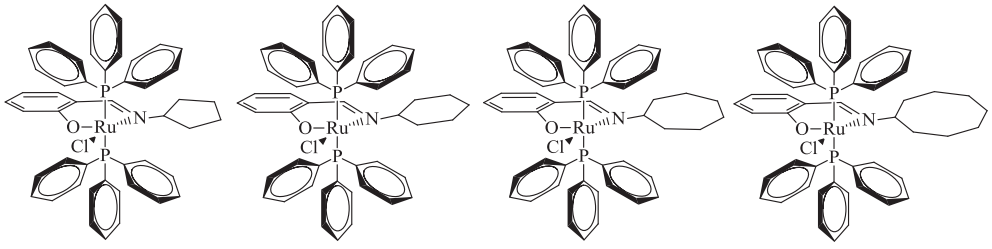

Fig. 1. Illustration of the Schiff base ruthenium(II) complexes (**2a-d**).

Schiff-Base Ligand **1b**: Salicylaldehyde (0.48 g, 4.0 mmol), cyclohexylamine (0.39 g, 4.0 mmol), and methanol (15 mL) afforded 0.68 g (85%) of the title compound as a yellow oil. Refractive index 1.5678; (a) UV–Vis: $\lambda_{max(n)}$ (nm), $\varepsilon_{max(n)}$ [M^{-1} cm^{-1}]: $\lambda_{max(1)}$ (317), $\varepsilon_{max(1)}$ [9700]; (b) IR (KBr): ν_x (cm^{-1}): νC = N (1629), νC–O (1274), (c) ^{1}H NMR: ($CDCl_3$, 400 MHz): 13.83 (s, 1H, OH), 8.37 (s, 1H, CH=N), 7.31–7.27 (dd, $^3J_{H,H}$ = 1.6 Hz, dd, $^3J_{H,H}$ = 0.8 Hz, 1H, salicyl-ring), 7.23–7.25 (dd, $^3J_{H,H}$ = 1.6 Hz, 1H, salicyl-ring), 6.94–6.98 (dt, $^3J_{H,H}$ = 6 Hz, $^3J_{H,H}$ = 0.4 Hz, 1H, salicyl-ring), 6.85–6.89 (td, $^3J_{H,H}$ = 0.8 Hz, 1H, salicyl-ring), 3.22–3.30 (m, 1H, CH^{Hexyl}), 1.80–1.87 (m, 4H, CH_2^{Hexyl}), 1.50–1.70 (m, 3H, CH_2^{Hexyl}), 1.27–1.45 (m, 3H, CH_2^{Hexyl}); ^{13}C NMR ($CDCl_3$) δ 162.1, 161.4, 131.9, 131.1, 118.9, 118.3, 117.04, 77.3, 77.02, 76.7, 67.4, 25.5, 24.3.

Schiff-Base Ligand **1c**: Salicylaldehyde (0.48 g, 4.0 mmol), cycloheptylamine (0.45 g, 4.0 mmol), and methanol (15 mL) afforded 0.69 g (80%) of the title compound as a yellow oil. Refractive index 1.5652; (a) UV–Vis: $\lambda_{max(n)}$ (nm), $\varepsilon_{max(n)}$ [M^{-1} cm^{-1}]: $\lambda_{max(1)}$ (316), $\varepsilon_{max(1)}$ [9600]; (b) IR (KBr): ν_x (cm^{-1}): νC = N (1621), νC–O (1270); (c) ^{1}H NMR: ($CDCl_3$, 400 MHz): 13.85 (s, 1H, OH), 8.3 (s, 1H, CH=N), 7.25–7.32 (dd, $^3J_{H,H}$ = 1.6 Hz, dd, $^3J_{H,H}$ = 0.8 Hz, 1H, salicyl-ring), 7.22–7.25 (dd, $^3J_{H,H}$ = 1.2 Hz, 1H, salicyl-ring), 6.95–6.98 (dt, $^3J_{H,H}$ = 6.4 Hz, $^3J_{H,H}$ = 0.4 Hz, 1H, salicyl-ring), 6.85–6.89 (td, $^3J_{H,H}$ = 0.8 Hz, 1H, salicyl-ring), 3.37–3.46 (m, 1H, CH^{Heptyl}), 1.82–1.90 (m, 2H, CH_2^{Heptyl}), 1.72–1.82 (m, 4H, CH_2^{Heptyl}), 1.50–1.70 (m, 6H, CH_2^{Heptyl}); ^{13}C NMR ($CDCl_3$) δ 161.66, 161.39, 131.92, 131.02, 118.91, 118.29, 116.99, 77.34, 77.08, 76.83, 70.12, 36.40, 28.54, 24.24.

Schiff-Base Ligand **1d**: Salicylaldehyde (0.48 g, 4.0 mmol), cyclooctylamine (0.51 g, 4.0 mmol), and methanol (15 mL) afforded 0.82 g (90%) of the title compound as a yellow oil. Refractive index 1.5631; (a) UV–Vis: $\lambda_{max(n)}$ (nm), $\varepsilon_{max(n)}$ [M^{-1} cm^{-1}]: $\lambda_{max(1)}$ (318), $\varepsilon_{max(1)}$ [10000]; (b) IR (KBr): ν_x (cm^{-1}): νC = N (1624), νC–O (1278); (c) ^{1}H NMR: ($CDCl_3$, 400 MHz): 13.85 (s, 1H, OH), 8.3 (s, 1H, CH=N), 7.27–7.32 (dd, $^3J_{H,H}$ = 1.2 Hz, dd, $^3J_{H,H}$ = 0.8 Hz, 1H, salicyl-ring), 7.22–7.25 (dd, $^3J_{H,H}$ = 1.2 Hz, 1H, salicyl-ring), 6.93–6.97 (dt, $^3J_{H,H}$ = 6.4 Hz, 1H, salicyl-ring), 6.84–6.88 (td, $^3J_{H,H}$ = 0.8 Hz, 1H, salicyl-ring), 3.40–3.45 (m, 1H, CH^{Octyl}), 1.75–1.90 (m, 6H, CH_2^{Octyl}), 1.45–1.70 (m, 8H, CH_2^{Octyl}); ^{13}C NMR ($CDCl_3$) δ 161.7, 161.4, 131.9, 131, 118.9, 118.3, 117.04, 77.3, 77, 76.8, 70, 51.4, 35.6, 33.47, 27.54, 25.48, 23.6.

2.4. General procedure for the preparation of Schiff-base Ru complexes (**2a-d**)

Synthesis of the ruthenium(II) Schiff base complexes (**2a**-**d**) was accomplished according to the following procedure: To a solution of Schiff base **1a-d** in methanol was added dropwise a solution of NaOH in methanol and the reaction mixture was stirred for 2 h at room temperature. The deprotonated ligand mixture was transferred by cannula to a 50-mL three-necked flask fitted with a reflux condenser containing the $[RuCl_2(PPh_3)_3]$ precursor, stirred mixture was refluxed for 4 h. A yellow precipitate was then filtered and washed with methanol and ethyl ether and then dried in a vacuum.

Complex **2a**: $[RuCl_2(PPh_3)_3]$ complex (0.30 g, 0.31 mmol), Schiff base **1a** (0.070 g, 0.37 mmol), NaOH (0.18 g, 0.45 mmol), and methanol (20 mL) afforded 0.25 g (80%) of the title complex as a yellow solid: anal. calculated for $C_{49}H_{48}ClNOP_2Ru$ was 68.01 C, 5.59 H and 1.62% N; found: 68.34C, 5.55 H and 1.60% N. UV–Vis: $\lambda_{max(n)}$ (nm), $\varepsilon_{max(n)}$ [M^{-1} cm^{-1}]: $\lambda_{max(1)}$ (252), $\varepsilon_{max(1)}$ [10020], $\lambda_{max(2)}$ (370), $\varepsilon_{max(2)}$ [625], $\lambda_{max(3)}$ (422), $\varepsilon_{max(3)}$ [240]; IR (KBr): ν_x (cm^{-1}): νC = N (1618), νC–O (1355); ^{1}H NMR: ($CDCl_3$, 400 MHz): 7.30–7.70 (m, 12H: *metha*-PPh_3 and 1H: CH=N), 7.30–7.70 (m, 6H, *para*-PPh_3), 7.21–7.30 (m, 12H, *ortho*-PPh_3), 6.63–6.68 (m, 1H, salicyl-ring), 6.4–6.5 (dd, $^3J_{H,H}$ = 1.6 Hz, dd, $^3J_{H,H}$ = 1.2 Hz, 1H, salicyl-ring), 6.04–6.10 (m, 1H, salicyl-ring), 5.85–5.80 (m, 1H, salicyl-ring), 3.85–3.92 (m, 1H, CH^{Pentyl}), 1.60–1.80 (m, 3H, CH_2^{Pentyl}), 1.29–1.38 (m, 4H, CH_2^{Pentyl}), 1.07–1.15 (m, 1H, CH_2^{Pentyl}),^{13}C NMR ($CDCl_3$) δ 166.12, 160.83, 135.16, 135, 134.84, 134.26, 134.21, 134.16, 132.12, 132.04, 131.93, 131.91, 129, 128.53, 128.44, 127.62, 127.59, 127.55, 123.36, 121.99, 111.80, 75.92, 32.39, 23.43; ^{31}P{^{1}H} NMR ($CDCl_3$: δ, ppm): 43.15 (s). EPR: no signal was observed.

Complex **2b**: $[RuCl_2(PPh_3)_3]$ complex (0.30 g, 0.31 mmol), Schiff base **1b** (0.075 g, 0.37 mmol), NaOH (0.18 g, 0.45 mmol), and methanol (20 mL) afforded 0.20 g (75%) of the title complex as a yellow solid: anal. calculated for $C_{50}H_{50}ClNOP_2Ru$ was 68.29 C, 5.73 H and 1.59% N; found: 68.41C, 5.64 H and 1.61% N. UV–Vis: $\lambda_{max(n)}$ (nm), $\varepsilon_{max(n)}$ [M^{-1} cm^{-1}]: $\lambda_{max(1)}$ (252), $\varepsilon_{max(1)}$ [10050], $\lambda_{max(2)}$ (369), $\varepsilon_{max(2)}$ [1766], $\lambda_{max(3)}$ (420), $\varepsilon_{max(3)}$ [585]; IR (KBr): ν_x (cm^{-1}): νC = N (1618), νC–O (1342); ^{1}H NMR: ($CDCl_3$, 400 MHz): 7.30–7.80 (m, 12H: *metha*-PPh_3 and 1H: CH=N), 7.30–7.80 (m, 6H, *para*-PPh_3), 7.08–7.30 (m, 12H, *ortho*-PPh_3), 6.57–6.67 (m, 1H, salicyl-ring), 6.38–6.51 (dd, $^3J_{H,H}$ = 1.2 Hz, dd, $^3J_{H,H}$ = 1.6 Hz, 1H, salicyl-ring), 5.99–6.12 (m, 1H, salicyl-ring), 5.76–5.89 (dd, *J* = 0.8 Hz, 1H, salicyl-ring), 3.18–3.33 (m, 1H, CH^{Hexyl}), 1.44–1.57 (m, 4H, CH_2^{Hexyl}), 0.78–1.05 (m, 4H, CH_2^{Hexyl}), 0.65–0.78 (m, 2H, CH_2^{Hexyl}); ^{13}C NMR ($CDCl_3$) δ 166.03, 160.74, 135.26, 135.10, 134.94, 134.22, 131.98, 128.99, 127.59, 123.40, 122.28, 111.68, 77.24, 76.99, 76.73, 73.17, 33.20, 26.03, 25.84; ^{31}P{^{1}H} NMR ($CDCl_3$: δ, ppm): 43.37 (s). EPR: no signal was observed.

Complex **2c**: $[RuCl_2(PPh_3)_3]$ complex (0.30 g, 0.31 mmol), Schiff base **1c** (0.080 g, 0.37 mmol), NaOH (0.18 g, 0.45 mmol), and methanol (20 mL) afforded 0.23 g (85%) of the title complex as a yellow solid: nal. calculated for $C_{51}H_{52}ClNOP_2Ru$ was 68.56 C, 5.87 H and 1.57% N; found: 69.19C, 5.64 H and 1.64% N; UV–Vis: $\lambda_{max(n)}$ (nm), $\varepsilon_{max(n)}$ [M^{-1} cm^{-1}]: $\lambda_{max(1)}$ (246), $\varepsilon_{max(1)}$ [9500], $\lambda_{max(2)}$ (370), $\varepsilon_{max(2)}$ [1268], $\lambda_{max(3)}$ (423), $\varepsilon_{max(3)}$ [599]; IR (KBr): ν_x (cm^{-1}): νC = N (1610), νC–O (1337); ^{1}H NMR: ($CDCl_3$, 400 MHz): 7.30–7.69 (m, 12H: *metha*-PPh_3 and 1H: CH=N), 7.30–7.69 (m, 6H, *para*-PPh_3), 6.92–7.30 (m, 12H, *ortho*-PPh_3), 6.60–6.73 (d, $^3J_{H,H}$ = 1.6 Hz, 1H, salicyl-ring), 6.47–6.56 (d, $^3J_{H,H}$ = 1.6 Hz, 1H, salicyl-ring), 6.09–6.20 (m, 1H, salicyl-ring), 5.73–5.85 (d, $^3J_{H,H}$ = 0.8 Hz, 1H, salicyl-ring), 3.63–3.77 (m, 1H, CH^{Heptyl}), 1.37–1.64 (m, 4H, CH_2^{Heptyl}), 1.27–1.36 (m, 4H, CH_2^{Heptyl}), 1.03–1.15 (m, 4H, CH_2^{Heptyl}); ^{13}C NMR ($CDCl_3$) δ 166.20, 161.6, 135.47, 135.30, 135.14, 134.24, 134.19, 134.14, 134.03, 132.13, 132.05, 131.96, 131.88, 128.97, 128.68, 128.52, 128.42, 127.64, 127.60, 127.56, 123.52, 122.78, 111.75, 75.0, 33.32, 26.6, 25.85, 25.02; ^{31}P{^{1}H} NMR ($CDCl_3$: δ, ppm): 42.48 (s). EPR: no signal was observed.

Complex **2d**: $[RuCl_2(PPh_3)_3]$ complex (0.30 g, 0.31 mmol), Schiff base **1d** (0.085 g, 0.37 mmol), NaOH (0.18 g, 0.45 mmol), and methanol (20 mL) afforded 0.21 g (75%) of the title complex as a yellow solid: anal. calculated for $C_{52}H_{54}ClNOP_2Ru$ was 68.82 C, 6.00 H and 1.54% N; found 69.03C, 6.21 H and 1.62% N. UV–Vis: $\lambda_{max(n)}$ (nm), $\varepsilon_{max(n)}$ [M^{-1} cm^{-1}]: $\lambda_{max(1)}$ (262), $\varepsilon_{max(1)}$ [10000], $\lambda_{max(2)}$ (377), $\varepsilon_{max(2)}$ [1528], $\lambda_{max(3)}$ (426), $\varepsilon_{max(3)}$ [822]; IR (KBr): ν_x (cm^{-1}): νC = N (1611), νC–O (1336); ^{1}H NMR: ($CDCl_3$, 400 MHz): 7.23–7.72 (m, 12H: *metha*-PPh_3 and 1H: CH=N), 7.23–7.72 (m, 6H, *para*-PPh_3), 6.95–7.23 (m, 12H, *ortho*-PPh_3), 6.60–6.67 (m, 1H, salicyl-ring), 6.52–6.58 (d, $^3J_{H,H}$ = 1.6 Hz, 1H, salicyl-ring), 6.09–6.16 (m, 1H, salicyl-ring), 5.76–5.80 (m, 1H, salicyl-ring), 3.62–3.76 (m, 1H, CH^{Octyl}), 1.38–1.50 (m, 4H, CH_2^{Octyl}), 1.30–1.36 (m, 4H, CH_2^{Octyl}), 1.05–1.25 (m, 6H, CH_2^{Octyl}); ^{13}C NMR ($CDCl_3$) δ 166.13, 161.78, 135.12, 134.19, 134.03, 132.12, 132.04, 131.93, 128.99, 128.53, 128.44, 127.61, 123.50, 122.80, 111.81, 77.25, 77.00, 76.74, 74.85, 33.31, 26.57, 25.84, 25.01; ^{31}P{^{1}H} NMR ($CDCl_3$: δ, ppm): 42.57 (s). EPR: no signal was observed.

2.5. ROMP procedure

In a typical ROMP experiment, 1.1 μmol of complex was dissolved in $CHCl_3$ (2 mL) with an appropriate amount of monomer

(NBE, 5.5 mmol) and additive (HCl, 27.5 μmol), followed by addition of carbene source (EDA, 43 μmol). Usually the solution gelled for 1–2 min, but the reaction mixture was stirred for 60 min at 25 or 50 °C in a silicon oil bath. At room temperature, 5 mL of methanol was added and the polymer was filtered, washed with methanol and dried in a vacuum oven at 40 °C up to constant weight. The reported yields are average values from catalytic runs performed at least three times with 10% error at the most. The isolated polyNBEs were dissolved in THF for GPC data.

2.6. ATRP procedure

In a typical ATRP experiment, 12.3 μmol of complex was placed in a Schlenk tube containing a magnet bar and capped by a rubber septum. Air was expelled by three vacuum–nitrogen cycles before appropriate amounts of monomer (MMA, 12.3 mmol), initiator (EBiB, 24.6 μmol), and DCE (1 mL) were added. All liquids were handled with dried syringes under nitrogen. The tube was capped under N_2 atmosphere using Schlenk techniques, then the reaction mixture was immediately immersed in an oil bath previously heated to the desired temperature. The polymerizations were conducted at 85 °C. The samples were removed from the tube after certain time intervals using degassed syringes. The polymerization was stopped when the reaction mixture became very viscous. The reported conversions are average values from catalytic runs performed at least twice.

3. Results and discussion

3.1. Synthesis and characterization

The bidentate Schiff bases (**1a-d**) were readily prepared by condensation of salicylaldehyde with four different cycloalkylamines in methanol (Scheme 1). When 1 mol of salicylaldehyde and 1 mol of amine were reacted, the corresponding products were obtained under mild conditions; confirmation of these products was demonstrated by spectroscopic data. As the ligands predominantly exist in the keto tautomeric form in the solid state. Prior to the complexation step an equivalent amount of NaOH in methanol was added to the ligands to convert this keto form to enolate form. This renders the coordination of enolate oxygen. Equimolar reactions between $[RuCl_2(PPh_3)_2]$ with the corresponding deprotonated Schiff bases (**1a-d**) led to the ruthenium(II) Schiff base complexes **2a-d** in high yields (Scheme 1).

In the ^1H NMR spectra in $CDCl_3$ for the synthesized ligands (**1a-d**) and their complexes (**2a-d**) are given in Section 2. The peaks in the range 1.0–2.0 ppm for ligands **1a-d** and 0.65–2.0 ppm for complexes **2a-d**, as multiplets, are assignable to the CH_2 groups hydrogens from the *N*-cycloalkyl substituent. Additionally, the peaks at range 6.84–7.32 ppm for ligands **1a-d** and 5.73–6.73 for complexes **2a-d**, as multiplets, are assignable to the protons of aromatic –C*H* groups. In the ^1H NMR spectra of ligands **1a-d** and complexes **2a-d**, the chemical shifts observed around 8.3 ppm for free ligands and at 7.22–7.50 for complexes **2a-d** as singlets are assigned to the proton of azomethine (–N=C*H*–) [15]. The peak due to the azomethine showed a high field shift compared to the free Schiff base after complexation with the metal ion indicating coordination through the azomethine nitrogen atom. A singlet for OH has a distinct down-field resonance at 13.8 ppm, characteristic for the acidic proton involved in a strong intramolecular hydrogen bond in the ligands **1a-d** [15]. These signals did not appear in the complexes **2a-d** as expected. The ^1H NMR spectra for the complexes **2a-d** were dominated by multiplets between 6.92 and 7.80 ppm due to the phenyl protons of two PPh_3 ligands coordinated in the Ru center which are upfield relative to the multiplets around 6.92–7.80 ppm from the aromatic signals for the Schiff base. In the ^{13}C NMR spectra, the carbon peaks between 23.6 and 161.6 ppm for ligands **1a-d** and 23.4–166.2 ppm for complexes **2a-d** were observed. ^{31}P NMR spectroscopy confirmed the presence of the PPh_3 ligands and their magnetic equivalence revealed that the two PPh_3 ligands are *trans*-positioned to each other in the complexes **2a-d** since only a singlet around 43 ppm was found for all complexes, thereby minimizing steric repulsion. This orientation is typical for ruthenium Schiff base complexes containing the *trans*-$[Ru(PPh_3)_2]$ core [16]. The FTIR spectra of the ligands **1a-d** were compared with that of the complexes **2a-d** in order to confirm the coordination of ligand to the ruthenium metal. The infrared spectra of free ligands show the characteristic ν(O–H) absorption bands around 2678 cm^{-1} which disappears after complexation, the absorption corresponding to the ν(C=N) vibration is around 1625 cm^{-1} in the ligands, and it is shifted approximately 12 cm^{-1} to a lower wavenumber in the spectra of the complexes **2a-d** confirming the coordination of azomethine nitrogen to the metal. The coordination of phenolic oxygen of the Schiff bases is supported by

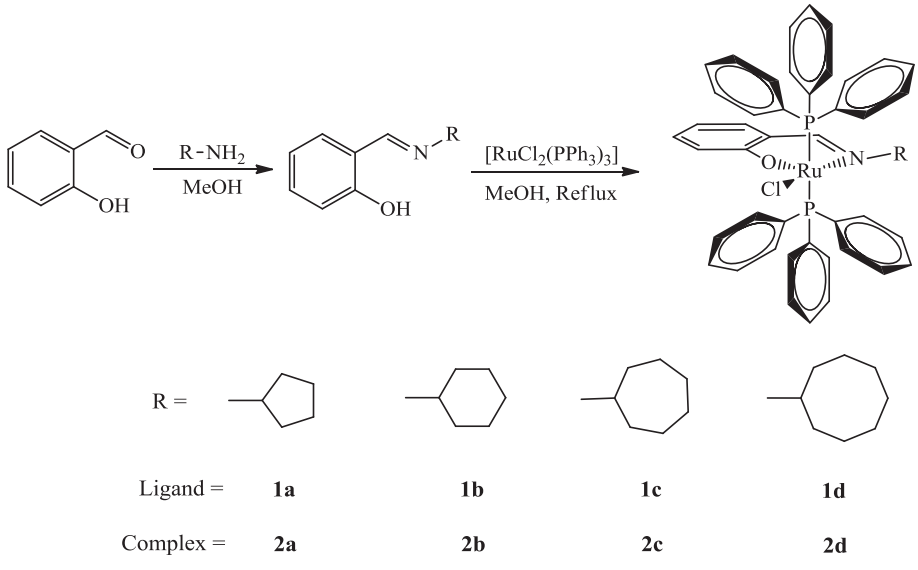

Scheme 1. Synthesis protocol of Schiff base **1a-d** and their ruthenium complexes **2a-d**.

the appearance of new bands in 497–499 cm^{-1} range due to ν(Ru–O) stretching in the ruthenium complexes [17]. In addition, these complexes exhibit one strong band in the range 414–417 cm^{-1}, which may be due to ν(Ru–N) stretching suggesting coordination of azomethine nitrogen atoms [17].

Electronic spectra of ligands **1a-d** and their complexes **2a-d** have been recorded in the 200–700 nm range in $CHCl_3$ and their corresponding data are given in Table 1. The formation of the complexes **2a-d** was also confirmed by electronic spectra (Fig. 2). In the electronic spectra of the free ligands and their complexes, the wide range bands were observed due to either the $\pi \rightarrow \pi^*$ and $n \rightarrow \pi^*$ of C=N chromophore or charge-transfer transition arising from π electron interactions between the metal and ligand, which involves either a metal-to-ligand electron transfer [18]. The electronic spectra of the ligands **1a-d** in $CHCl_3$ (Fig. 3) showed strong absorption bands in the ultraviolet region (316–318 nm), that could be attributed respectively to the $\pi \rightarrow \pi^*$ and $n \rightarrow \pi^*$ transitions in the benzene ring or azomethine (–C=N) groups [19]. In the electronic spectra of the complexes **2a-d**, these bands show hypsochromic shifts relative to their free ligands, and they may be hidden under the electronic transition of the PPh_3 ligands. This displacement of the absorption bands of the complexes **2a-d** most likely originate from the metalation which increases the conjugation and delocalization of the whole electronic system and results in the energy change of the intra-ligand transitions of the conjugated chromophore. These results clearly indicate that the ligand coordinates to metal center, which are in accordance with the results of the other spectroscopic data. Furthermore, the absorption bands in the visible region are observed at between 360 and 426 nm as a low intensity bands These bands are considered to arise from the MLCT transition [20].

The electrochemical activity of the complexes **2a-d** was studied by cyclic voltammetry in scan rate of 100 mV s^{-1} in CH_2Cl_2 solution containing 0.1 M *n*-Bu_4NPF_6 supporting electrolyte in the potential range 0–1.1 V. The cyclic voltammograms of **2a-d** are shown in Fig. 3 and the voltammetric data are summarized in Table 2. On scanning anodically and reversing the scan direction, similar anodic waves which may be attributed to the $Ru^{II/III}$ redox couple and the redox-active phenolate moieties were observed between 0.41 and 0.60 V and 0.7–1.0, respectively, for all Schiff base Ru complexes (Fig. 3). Less intense corresponding cathodic peaks were observed; and this may be attributed to the instability and transient nature of the Ru^{III} ions in solution. Overall there is a clear shift in the redox potentials towards more negative values as the electron-donating ability of the cycloalkyl substituents is increased (Octyl > Heptyl > Hexyl > Pentyl). Modulation of the electron-donating ability, as well as the steric effect of the Schiff base ligands is subsequently shown to have an effect on the activity on ROMP and ATRP of the complexes **2a-d**.

Table 1
Infrared and electronic absorption data for base Schiff ligands **1a-d** and their ruthenium complexes **2a-d**.

Compounds	FTIR (cm^{-1})		UV-Vis (nm)	
	Ligand	Complex	Ligand	Complex
1a/2a	1277 ν(C-O) 1629 ν(C=N) 2734 ν(O-H) 2952 ν(C-H)	416 ν(Ru-N) 499 ν(Ru-O) 1355 ν(C-O) 1618 ν(C=N)	317 ($\pi \rightarrow \pi^*$)	252 ($\pi \rightarrow \pi^*$) 313 ($n \rightarrow \pi^*$) 370 (MLCT) 422 (MLCT)
1b/2b	1274 ν(C-O) 1629 ν(C=N) 2663 ν(O-H) 2925 ν(C-H)	417 ν(Ru-N) 497 ν(Ru-O) 1342 ν(C-O) 1618 ν(C=N)	317 ($\pi \rightarrow \pi^*$)	252 ($\pi \rightarrow \pi^*$) 313 ($n \rightarrow \pi^*$) 369 (MLCT) 420 (MLCT)
1c/2c	1270 ν(C-O) 1621 ν(C=N) 2662 ν(O-H) 2910 ν(C-H)	416 ν(Ru-N) 497 ν(Ru-O) 1337 ν(C-O) 1610 ν(C=N)	316 ($\pi \rightarrow \pi^*$)	246 ($\pi \rightarrow \pi^*$) 273 ($n \rightarrow \pi^*$) 370 (MLCT) 423 (MLCT)
1d/2d	1278 ν(C-O) 1624 ν(C=N) 2651 ν(O-H) 2904 ν(C-H)	414 ν(Ru-N) 498 ν(Ru-O) 1336 ν(C-O) 1611 ν(C=N)	318 ($\pi \rightarrow \pi^*$)	262 ($\pi \rightarrow \pi^*$) 320 ($n \rightarrow \pi^*$) 377 (MLCT) 426 (MLCT)

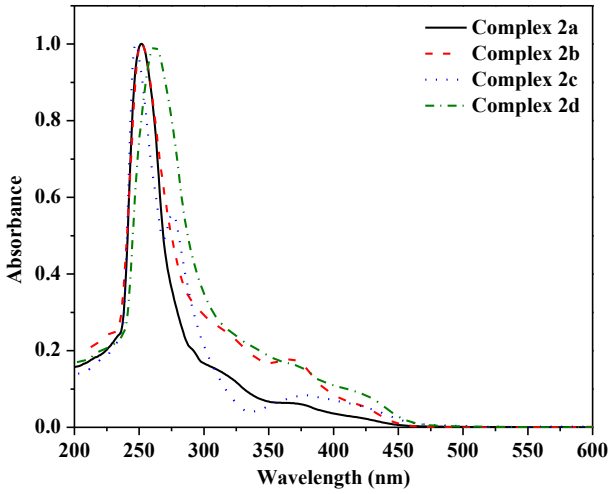

Fig. 2. Electronic spectra of the complexes **2a-d** in degassed CH_2Cl_2 solution at room temperature ([Ru] = 0.1 mmol L^{-1}).

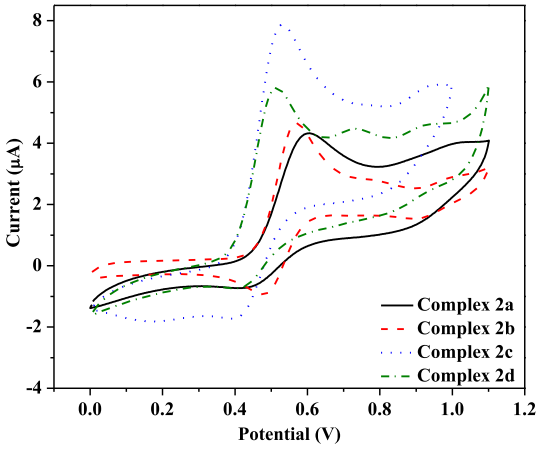

Fig. 3. Cyclics voltammograms of **2a-d** in CH_2Cl_2 at 25 °C. [Ru] = 10 mM; [*n*-Bu_4NPF_6] = 0.1 M. Scanning anodically from 0.0 up to 1.1 V at scan rates of 100 mV s^{-1}.

Table 2
Cyclic voltammetry[a] results for complexes **2a-d**.

Complex	CV			
	E_{pa} (V)	E_{pc} (V)	$E_{1/2}$ (V)	ΔE_p (V)
2a	0.599	0.462	0.530	0.137
2b	0.568	0.483	0.525	0.085
2c	0.529	0.408	0.468	0.121
2d	0.515	0.433	0.474	0.082

[a] Conditions: CH_2Cl_2, *n*-Bu_4NPF_6 (supporting electrolyte, 0.1 mol L^{-1}), [Ru] = 5 mmol L^{-1}, scan rate = 100 mV s^{-1}), platinum disk and wire (working and auxiliary electrode), Ag/AgCl (reference electrode). $E_{1/2}$ is the half-potential for the complex; ΔE_p is the cathodic-anodic peak separation.

3.2. ROMP reactions

The reactivity of the complexes **2a-d** as catalytic precursors was

tested on ROMP of NBE in $CHCl_3$ with [NBE]/[Ru] = 5000, volume of EDA = 5 μL at 25 °C for 60 min (Fig. 4). In general, the complexes **2a-d** presented low yields of polyNBE, the complex **2a** with lower yield of 4% and **2d** with higher yield equal to 11% (Table 3). ROMP of NBE with complexes **2a-d** was also evaluated at 50 °C under the same conditions. The increase of temperature produced higher yields of polyNBE, with maximum yields of up to 25% and PDI values between 1.1 and 2.3. As the temperature increased to 50 °C, the yields practically doubled with a significant increase in M_n values of the order from 10^3 to 10^4 g mol^{-1} in relation to 25 °C. When comparing the reactivity at 25 and 50 °C, the main difference was in the yields of polymer, which the catalytic activity at 50 °C was always higher than that observed at 25 °C for all complexes. Thus, the improvement in the catalytic activity of the complexes **2a-d** at 50 °C shows that the induction period was favored.

In order to optimize the induction period of the complexes **2a-d** in the ROMP mechanism, a chemical activation of the catalytic precursors was attempted with the use of HCl acid. This strategy has already been applied for the activation of ruthenium(II) Schiff bases catalysts, which the acid protonates the *N*-atom of the azomethine group [13c]. This causes the partial labilization of the Schiff base with generation of a vacancy at the ruthenium center, and the initiation step occurs as monomer is added. The ROMP of NBE catalyzed by the complexes **2a-d** in the presence of HCl is shown in Fig. 4, where the [HCl]/[Ru] ratio was investigated to find the optimal concentration of acid.

The catalytic activity of the complexes **2a-d** was sensitive with variation of the [HCl]/[Ru] molar ratio at 25 and 50 °C (Table 3). At 25 °C, a considerable increase in the yields of polyNBE as increasing the [HCl]/[Ru] ratio up to 25 was observed, followed by a drop for [HCl]/[Ru] ≥ 50. When polymerization was performed at 50 °C in the presence of acid, a similar profile was observed, although, higher values of polyNBE yields were achieved with M_n values near the order of 10^5 g mol^{-1}. It is rationalized that this increase in the catalytic activity of **2a-d** can be explained by the protonation of *N*-atom of the Schiff base azomethine group, it creates a vacant site at the ruthenium center to formation of active species. In addition, the steric hindrance in the different Schiff bases plays a decisive role in the reactivity in the complexes **2a-d**. Besides that, the order of reactivity of the complexes in ROMP increases from **2a** to **2d**. The lability of the azomethine group becomes more favored as the steric hindrance increases, as cycloalkyl substituent is increased from cyclopentyl (**2a**) to cyclooctyl (**2d**). However, excess HCl acid ([HCl]/[Ru] ≥ 50) in the mixture conducted a decreasing in the polyNBE yields. Perhaps, with a very excessive amount of HCl, the chlorides should compete for a coordination site and be able to

Table 3
Yield values and SEC data from the ROMP of NBE with **2a-d** at 25 and 50 °C; [NBE]/[Ru] = 5000 and 5 μL of EDA with 1.1 μmol of complex in CH_2Cl_2 for 60 min.

Complex	[HCl]/[Ru]	25 °C			50 °C		
		Yield (%)	M_n (10^3)	PDI	Yield (%)	M_n (10^3)	PDI
2a	0	4	4.1	1.2	8	98.8	2.3
	10	22	38.2	1.5	34	94.0	3.0
	25	29	49.2	1.2	43	87.3	1.3
	50	21	78.6	1.2	38	62.1	1.2
	150	16	60.2	1.4	24	97.0	3.7
	300	6	5.4	2.9	15	15.0	2.0
2b	0	4	8.7	1.1	10	86.0	1.1
	10	25	46.0	3.8	37	19.3	1.5
	25	28	68.0	3.8	43	49.2	3.2
	50	17	79.5	1.1	17	76.4	1.1
	150	18	56.4	3.2	18	54.4	1.2
	300	14	9.6	1.0	13	76.5	1.1
2c	0	8	2.4	2.0	15	68.0	1.3
	10	26	37.2	2.6	32	60.0	3.6
	25	31	64.5	2.3	43	32.5	1.6
	50	14	48.9	3.8	23	70.8	1.5
	150	11	61.2	3.1	18	71.0	1.1
	300	0	–	–	11	94.6	1.1
2d	0	11	54.0	1.1	25	96.1	1.1
	10	31	56.6	2.6	35	48.4	3.1
	25	34	10.8	3.0	44	72.6	1.1
	50	21	23.1	1.4	45	83.7	1.3
	150	13	34.5	2.7	36	90.1	2.8
	300	0	–	–	2	7.7	1.1

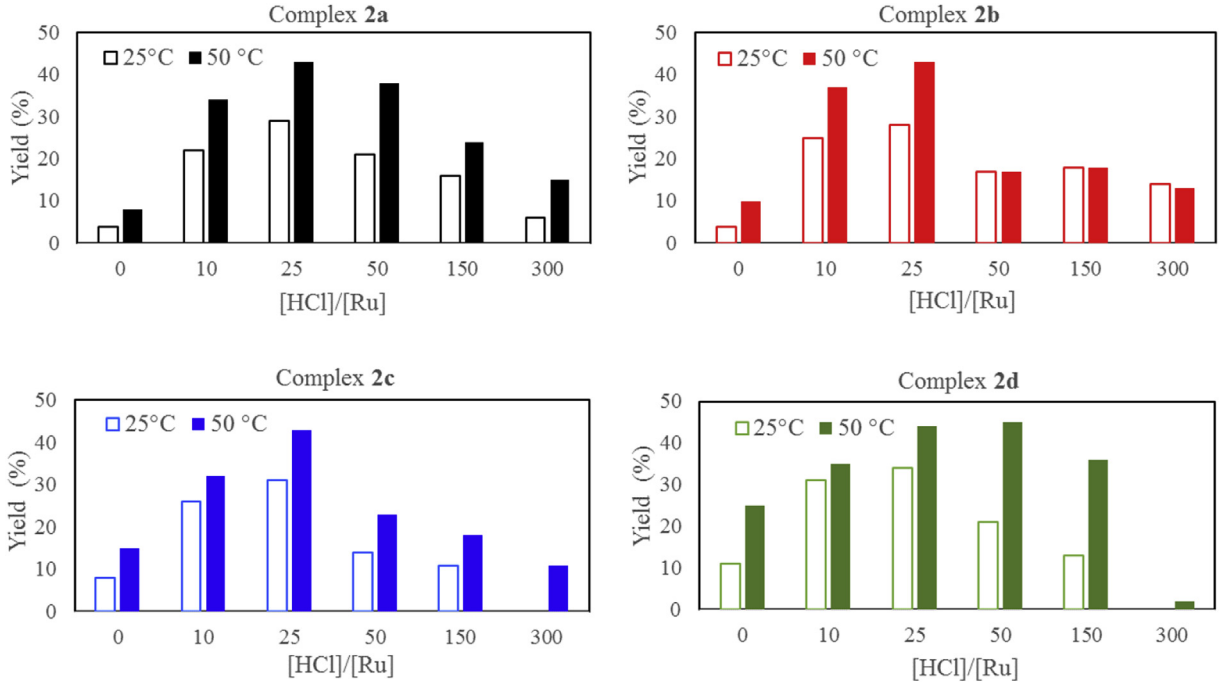

Fig. 4. Dependence of yield on the [HCl]/[Ru] molar ratio for ROMP of NBE with **2a-d**; [NBE]/[Ru] = 5000 and 5 μL of EDA in CH_2Cl_2 at 25 and 50 °C for 60 min.

coordinate to the ruthenium center, causing the degradation of the complex in solution by full release of the Schiff base of the coordinating sphere.

ROMP of NBE with the complexes **2a-d** was conducted varying the volume of EDA (Fig. 5), the polymerizations were carried out by keeping the optimal concentration of acid found ([HCl]/[Ru] = 25) at 25° C. No formation of polymer was observed in the absence of EDA. An increase in polyNBE yields is observed by increasing the volume of EDA up to 5 μL. For higher volumes of EDA (≥10 μL), a decreasing in yields is observed. In general, the M_n values also follow this trend with an increase of the molecular weights up to 5 μL followed by decreases to higher volumes of EDA (≥10 μL) with PDI values ranging from 1.1 to 3.0. (Table 4). The increase of polyNBE yields with increasing volume of EDA up to 5 μL is indicative of the coordination of EDA with associative character. However, it should be noted that a very excessive amount of EDA (≥10 μL) provokes a decreasing in the yields values, probably due to competition with the monomer for coordination onto the initiator active sites. Thus, it worth to mention that the optimum EDA amount used as a carbene source was of 5 μL for the complexes **2a-d**. Considering that these complexes have the same profile when reacted with EDA, it is possible to affirm that the four complexes have the same pathway in the formation of Ru carbene in the induction period.

The yields increase when increasing the [NBE]/[Ru] molar ratio starting from 3000 with yields of 5, 8, 12, and 15% with **2a**, **2b**, **2c**, and **2d**, respectively, reaching yields at least twice higher at 5000 for all complexes (Table 5). ROMP is a process governed by thermodynamic equilibrium, where the increase of monomer concentration favors the thermodynamic of polymerization providing higher polymer production [21].

When comparing the catalytic activity of the complexes in ROMP reactions, it is interesting to point out that the reactivity follows this order: **2a** < **2b** < **2c** < **2d**. The electronic and steric characteristics of the Schiff base ligands were able to tune the catalytic activity of complexes for ROMP of NBE, highlighting the importance of the Schiff base as ancillary ligand. However, it is reasonable to attribute that the steric effects on the Schiff base play a determinant role for the release of the azomethine group, rate-determining step for the formation of in-situ active species. Furthermore, this induction period can be faster as using acid (HCl).

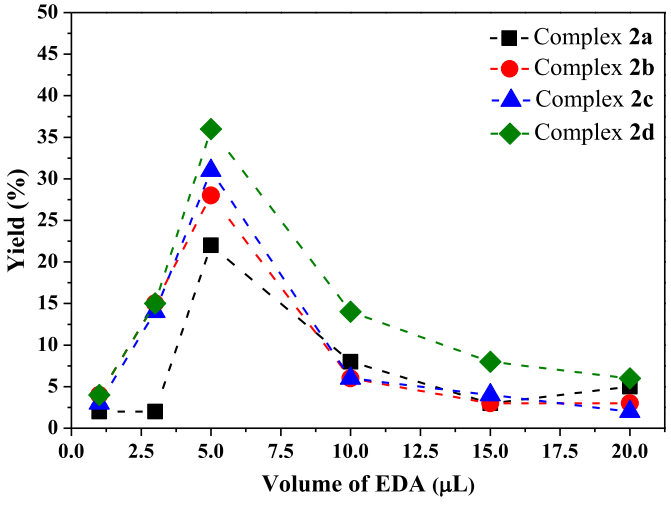

Fig. 5. Dependence of yield on the volume of EDA for ROMP of NBE with **2a-d**; [NBE]/[HCl]/[Ru] = 5000/25/1 with 1.1 μmol of complex in CH_2Cl_2 at 25 °C for 60 min.

Table 4
Yield values and SEC data from the ROMP of NBE with **2a-d** at 25 °C; [NBE]/[HCl]/[Ru] = 5000/25/1 with 1.1 μmol of complex in CH_2Cl_2 for 60 min.

Complex	Volume of EDA	Yield (%)	M_n (10^3)	PDI
2a	1	2	5.6	1.1
	3	2	6.8	1.2
	5	22	49.2	1.2
	10	8	7.9	1.2
	15	3	6.8	1.3
	20	5	8.1	1.3
2b	1	4	6.8	1.2
	3	15	71.2	1.2
	5	28	68.0	1.8
	10	6	21.8	1.2
	15	3	7.0	1.5
	20	3	8.9	1.4
2c	1	3	7.2	1.3
	3	14	62.2	1.2
	5	31	64.5	2.3
	10	6	7.4	1.4
	15	4	7.7	1.2
	20	2	7.4	1.1
2d	1	4	5.9	1.1
	3	15	60.7	1.1
	5	36	10.8	3.0
	10	14	76.5	1.1
	15	8	19.6	1.2
	20	6	7.9	1.2

Table 5
Yield values and SEC data from the ROMP of NBE with **2a-d** at 25 °C; [HCl]/[Ru] = 25/1 and 5 μL of EDA with 1.1 μmol of complex in CH_2Cl_2 for 60 min.

Complex	[NBE]/[Ru]	Yield (%)	M_n (10^3)	PDI
2a	3000	5	70.4	1.2
	5000	22	49.2	1.2
2b	3000	8	73.4	1.3
	5000	28	68.0	1.8
2c	3000	12	72.7	1.4
	5000	31	64.5	2.3
2d	3000	15	69.8	1.2
	5000	36	10.8	3.0

From the UV-Vis experiments, the kinetic constants of the reaction of the complexes **2a-d** with HCl acid ([HCl]/[Ru] = 25) was calculated (Fig. 6). The deprotonation reaction of the azomethine group was pseudo-first order with apparent rate constants (k_{obs}) of 2.7×10^{-4}, 4.5×10^{-4}, 6.4×10^{-4}, and 2.5×10^{-3} s^{-1} to the complex **2a**, **2b**, **2c**, and **2d**, respectively. A decrease in the k_{obs} values with the increase of the cycloalkyl substituent is observed; it confirms that the reaction between the complexes **2a-d** with the HCl acid is kinetically favored as the steric hindrance is increased.

Based on this, it is possible to infer that the difference in the reactivity of the studied complexes is directly related to the steric characteristics of the Schiff base ligands, which are modulated by their substituents. Upon metal-carbene formation, a PPh_3 leaves the complex, followed by the coordination of NBE to the carbene-Ru species. In order to confirm this proposal, experiments in the presence of excess PPh_3 (20 equiv.) at 25 °C for 60 min with [NBE]/[HCl]/[Ru] = 5000/25/1 and 5 μL of EDA for the complexes **2a-d**, which no formation of polymer was observed. This procedure confirms that the ROMP reaction did not occur, although the carbene complex formation took place. The ROMP will only occur when the PPh_3 molecule undergoes discoordination from the metal center (Scheme 2).

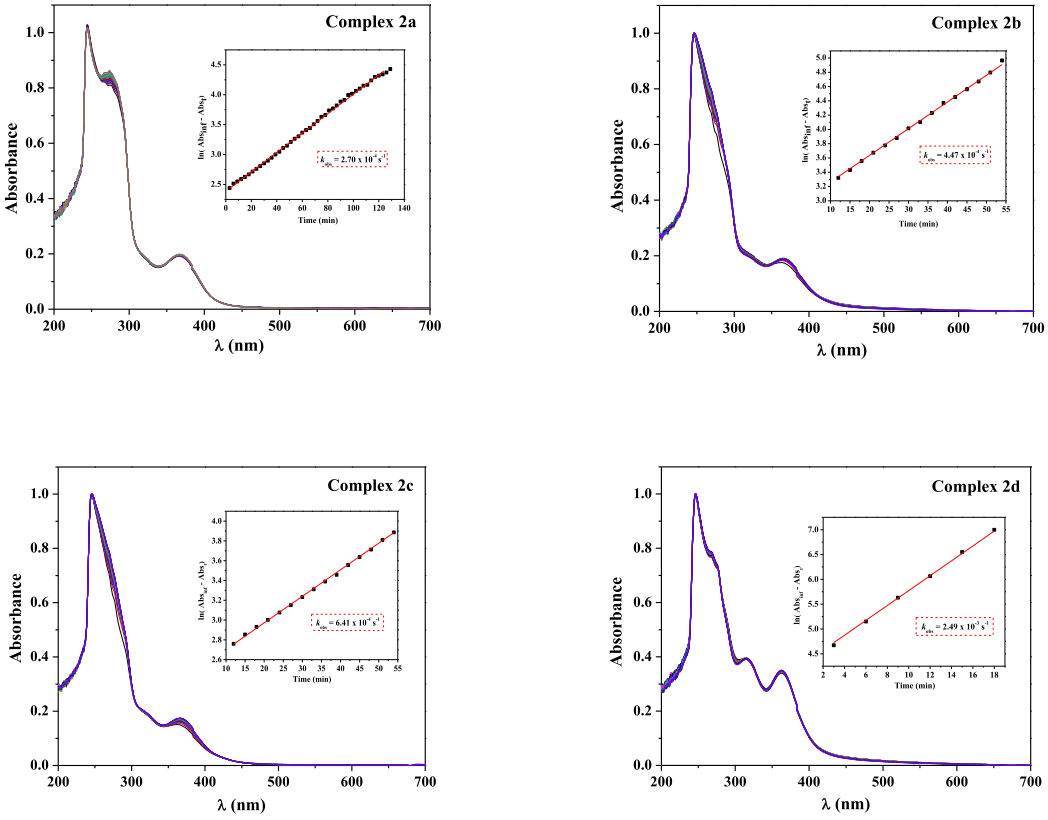

Fig. 6. Time-dependent UV-vis absorption spectra of **1**, **2**, and **3** in the presence of HCl in CH_2Cl_2 at 25 °C; [Ru] = 0.1 mmol L^{-1}); [HCl]/[Ru] = 25. *Insert*: Dependence of $\ln(A_{inf}\text{-}A_t)$ on the reaction time at 365 nm.

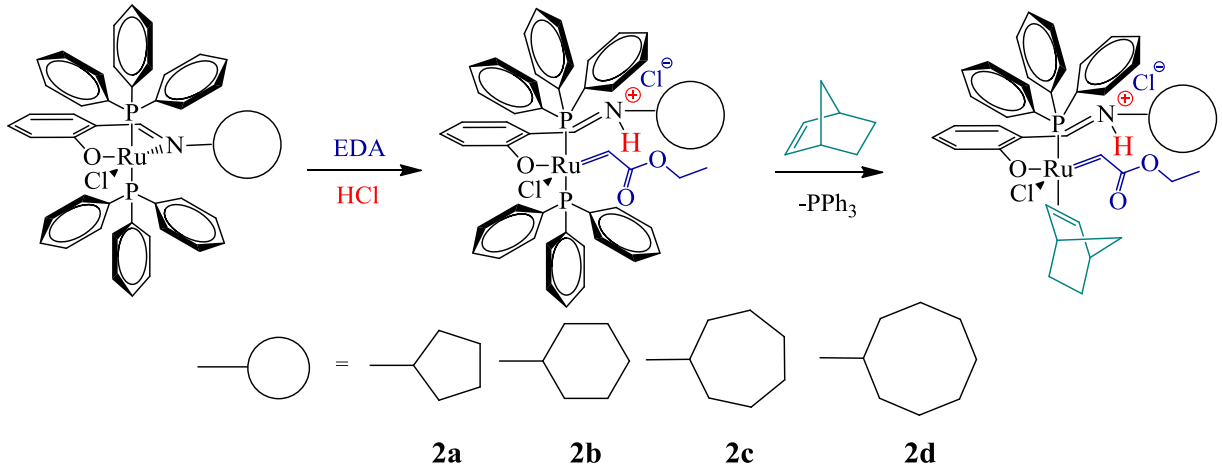

Scheme 2. Illustration of possible reaction steps for ROMP of NBE with the complexes **2a**-**d**.

3.3. ATRP reactions

The complexes **2a**-**d** have properties that make them promising reagents for use as ATRP catalysts. They provide reversible or quasi-reversible Ru^{II}/Ru^{III} couples at easily accessible potentials, as shown by the electrochemical data. They have either a vacant coordination site, which makes it possible for a halide ligand to enter the coordination sphere. Thus, MMA polymerization via ATRP with complexes **2a**-**d** were performed as a function of time using EB*i*B as initiator with [MMA]/[EBiB]/[Ru] = 1000/2/1 M ratio at 85° C. The MMA conversion values increase exponentially as a function of time in all cases (Fig. 7). MMA polymerization with **2a** achieved a maximum conversion of 47% of polyMMA and, when catalyzed by **2b**, the conversion was increased by 20%, reaching approximately 70% in 17 h. However, a decrease in conversion values was observed for the complexes **2c**-**d** under the same conditions.

Kinetics studies of MMA polymerization mediated by the complexes **2a**-**d** show a linear correlation of $\ln([MMA]_0/[MMA])$ as a

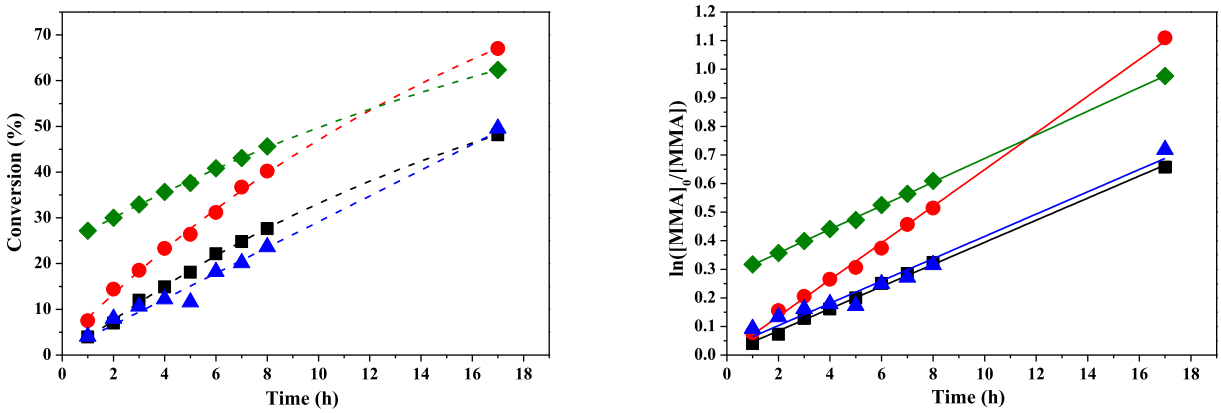

Fig. 7. Dependence of conversion and ln([MMA]$_0$/[MMA]) on the reaction time for ATRP of MMA with **2a** (■), **2b** (●), **2c** (▲) and **2d** (▼); [MMA]/[EBiB]/[Ru] = 1000/2/1 with 12.3 μmol of complex in CH_2Cl_2 at 85 °C.

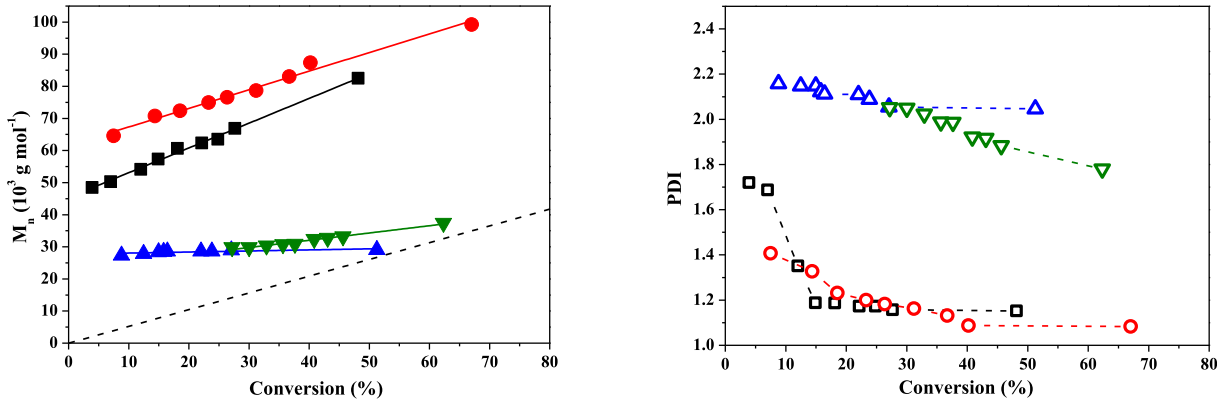

Fig. 8. Dependence of M_n and PDI on the conversion for ATRP of MMA with **2a** (■), **2b** (●), **2c** (▲) and **2d** (▼), [MMA]/[EBiB]/[Ru] = 1000/2/1 with 12.3 μmol of complex in CH_2Cl_2 at 85 °C.

function of time (Fig. 7), with a pseudo-first order rate constant (k_{obs}) equal to 1.07 × 10^{-5}, 1.78 × 10^{-5}, 1.08 × 10^{-5} and 1.15 × 10^{-5} s^{-1} for **2a**, **2b**, **2c** and **2d**, respectively. The linear semilogarithmic plot of ln[MMA]$_0$/[MMA]t versus time and the linear increase of molecular weight with conversion, in conjunction with moderate PDIs, illustrates a certain level of control imparted by the complexes **2a-b** (Figs. 7 and 8). However, in repeated kinetic experiments molecular weights were observed to be somewhat higher than the theoretical values. This can be attributed to the number of growing radical chains being lower than expected, resulting in an effective increase in the monomer concentration (f = 0.30–0.35). On the other hand, the molecular weight of poly-MMA obtained with **2c-d** showed non-dependence of the molecular weight on the conversion, coupled with PDI of ca. 2.0 clearly illustrating the lack of control during the polymerization. As observed, MMA polymerization suggests that the level of control can be slightly tuned by the substitution pattern of the ancillary ligand in the complexes **2a-d**, as more sterically hindered substituents were incorporated into the base Schiff ligand, polymerization control decreased.

4. Conclusion

The Schiff bases ligands **1a-d** and their respective complexes **2a-d** were successfully synthesized. The Schiff base-Ru^{II} complexes **2a-d** were characterized by FTIR, UV-Vis, ^{1}H-, ^{13}C and ^{31}P NMR, and cyclic voltammetry. Complexes **2a-d** were moderately active as catalytic precursors in ROMP of NBE and their catalytic activity was improved in the presence of the HCl acid using [NBE]/[HCl]/[Ru] = 5000/25/1 ratio in the presence of 5 μL of EDA for 60 min. The kinetic studies were determinate to explain the reactivity difference between the complexes **2a-d** against the ROMP reactions, it follows this order: **2a** < **2b** < **2c** < **2d**. The catalytic activity of the complexes **2a-d** suggests that the steric effects on the Schiff base play a determinate role for the release of the azomethine group, rate-determining step for the formation of in-situ active species, and this induction period can be faster as using acid (HCl).

MMA polymerization mediated by complexes **2a-d** was performed using [MMA]/[EBiB]/[Ru] = 1000/2/1 M ratio at 85 °C. A linear correlation of ln([MMA]$_0$/[MMA]) as a function of time mediated by complexes **2a-d** indicates some level of control in the polymerization as compared to conventional radical polymerization. However, better control levels were achieved with the complexes **2a-b**, in which the molecular weights increased linearly with the conversion with narrow polydispersity. On the other hand, complexes **2c-d** showed low efficiency in the control of MMA polymerization, evidenced by non-dependence of the molecular weight on the conversion and broad PDIs. It is believed that the steric hindrance of the Schiff base played a decisive role in the reactivity/efficiency against the controlled polymerization of MMA.

Acknowledgements

The authors are indebted to the financial support from FAPESP

(Proc. 2013/10002-0).

Appendix A. Supplementary data

Supplementary data related to this article can be found at https://doi.org/10.1016/j.jorganchem.2017.09.043.

References

[1] A.M. Abu-Dief, I.M.A. Mohamed, Beni-Suef Univ. J. Basic Appl. Sci. 4 (2015) 119–133.
[2] A. Prakash, D. Adhikari, Int. J. ChemTech Res. 3 (2011) 1891–1896.
[3] P.G. Cozzi, Chem. Soc. Rev. 33 (2004) 410–421.
[4] R.M. Clarke, T. Storr, Dalton Transac 43 (2014) 9380–9391.
[5] K.C. Gupta, A.K. Sutar, Coord. Chem. Rev. 252 (2008) 1420–1450.
[6] R. Drozdzak, B. Allaert, N. Ledoux, I. Dragutan, V. Dragutan, F. Verpoort, Adv. Synth. Catal. 347 (2005) 1721–1743.
[7] R.G. Cavell, K. Aparna, R.P. Kamalesh Babu, Q. Wang, J. Mol. Catal. A. Chem. 189 (2002) 137–143.
[8] S. Matsui, T. Fujita, Catal. Today 66 (2001) 63–73.
[9] Y. Nakayama, H. Bando, Y. Sonobe, T. Fujita, J. Mol. Catal. A. Chem. 213 (2004) 141–150.
[10] a) Marcus Seitz, G. Helmut, Alt J. Mol. Catal. A Chem. 257 (2006) 73–77;
b) R. Souane, F. Isel, F. Peruch, P.J. Lutz, Comptes Rendus Chim. 5 (2002) 43–48.
[11] a) Jing Wang, Xinli Zhang, Lu Zhou, Yang Zhou, Qigu Huang, Wantai Yang, J. Appl. Polym. Sci. 132 (2015) 42225;
b) Kefeng Liu, Gang Yao, Wenlei Wu, Bo Gao, Chem. Res. Chin. Univ. 30 (5) (2014) 825–830;
c) M. Mandal, D. Chakraborty, V. Ramkumar, RSC Adv. 5 (36) (2015) 28536–28553;
d) K. Liu, G. Yao, W. Wu, B. Gao, Chem. Res. Chin. Univ. 30 (5) (2014) 825–830.
[12] M.A. Mekewi, Int. J. Polym. Mater. 55 (2006) 219–234.
[13] a) R. Drozdzak, B. Allaert, N. Ledoux, I. Dragutan, V. Dragutan, F. Verpoort, Coord. Chem. Rev. 249 (2005) 3055–3074;
b) R. Drozdzak, B. Allaert, N. Ledoux, I. Dragutan, V. Dragutan, F. Verpoort, Adv. Synth. Catal. 347 (2005) 1721–1743;
c) Stijn Monsaert, Nele Ledoux, Renata Drozdzak, Francis Verpoort, J. Polym. Sci. Part A Polym. Chem. 48 (2010) 302–310;
d) Nele Ledoux, Renata Drozdzak, Bart Allaert, Anthony Linden, Pascal Van Der Voort, Francis Verpoort, Dalton Trans. (2007) 5201–5210;
e) Renata Drozdzak, Naoki Nishioka, Gilles Recher, Francis Verpoort, Macromol. Symp. 293 (2010) 1–4.
[14] a) P.W. Armit, A.S.F. Boyd, T.A. Stephenson, J. Chem. Soc. Dalton (1975) 1663;
b) P.R. Hoffman, K.G. Caulton, J. Am. Chem. Soc. 97 (1975) 4221;
c) R.C.J. Vriends, G.V. Koten, K. Vrieze, Inorg. Chim. Acta 26 (1978) L29.
[15] M.S. Refat, M.Y. El-Sayed, A. Majid, A. Adam, J. Mol. Struc. 1038 (2013) 62–72.
[16] K.P. Balasubramanian, K. Karvembu, R. Prabhakaran, V. Chinnusamy, K. Natarajan, Spectrochim. Acta, Part A. 68 (2007) 50.
[17] K. Nakamoto, Infrared and Raman Spectra of Inorganic and Coordination Compounds, fourth ed., John Wiley and Sons, Inc., New York, 1986.
[18] M.V. Kaveri, R. Prabhakaran, R. Karvembu, K. Natarajan, Spectrochim. Acta Part A 61 (2005) 2915.
[19] A. Böttcher, T. Takeuchi, K.I. Hardcastle, T.J. Meade, H.B. Gray, D.C. Wikel, M. Kapon, Z. Dori, Inorg. Chem. 36 (1997) 2498.
[20] a) K. Natarajan, R.K. Poddar, C. Agarwala, Oxford, J. Inorg. Nucl. Chem. 39 (3) (1997) 431;
b) A.B.P. Lever, Inorganic Electronic Spectroscopy, second ed., Elsevier, Amsterdam, The Netherlands, 1984;
c) K. Chichak, U. Jacquenard, N.R. Branda, Weinheim, Eur. J. Inorg. Chem. 2002 (2) (2002) 357.
[21] C.W. Bielawski, R.H. Grubbs, Prog. Polym. Sci. 32 (2007) 1–29.